Low Energy Photonuclear Reactions: Photofission and Photon Scattering Experiments*

Ulrich Kneissl
Institut fur *Strahlenphysik, Universität* Stuttgart
D-70569 Stuttgart, Germany

Received September 12, 1993

Two topics, photofission and photon scattering experiments, are emphasized and described in more detail in this report on low energy photonuclear reactions. The essential experimental progress achieved during the last years is summarized. It is mainly based on the advent of modern high duty cycle and high current electron accelerators and improved detector systems (4a fragment detectors, high resolution γ-spectrometers and polarimeters). Novel results are presented. Fragment angular distributions in $(e,e'f)$-coincidence experiments allowed to disentangle all six low lying transitions states in ^{238}U. By simultaneous measurements of both fragment mass and angular distributions, the coupling of the Bohr transition states to diverse fission modes (Brosa modes) could be studied and a mass dependence of fission fragment angular distributions could be established. Furthermore, these measurements of fragment angular distributions for separated fragment masses allow to detect contributions of odd harmonics in the angular distributions due to $E1/E2$ interferences. Linearly *polarized* photons were used as a new tool to search for $M1$ contributions in the near barrier photofission. In first photofission experiments using monochromatic tagged photons the second chance fission of ^{238}U was investigated. The results provided spin and I<-number assignments to low lying transition states in the unstable nucleus ^{237}U. Systematic low energy photon scattering experiments (nuclear resonance fluorescence experiments) provided unique informations on low lying magnetic and electric dipole excitations in heavy nuclei. Precise excitation energies, transition widths, spins, K-numbers and parities of numerous states in heavy nuclei could be determined. The systematics and strength fragmentation of the orbital $M1$ mode, the so called *"Scissors Mode"* in deformed rare earth and actinide nuclei could be established. The linear increase of the total $M1$ strength with the square of the deformation parameter β_2 could be confirmed. For the first time the Scissors Mode excitation could be detected in an odd mass nucleus (^{163}Dy). On the other hand, low lying electric $\Delta K = 0^-$-transitions of remarkable strengths have been observed in all investigated even deformed nuclei near 1.5 MeV. These 1^- states are discussed in terms of a $K = 0$ rotational band based on an octupole vibration. The surprising novel result of the recent systematic polarization studies, however, was the first observation of enhanced electric dipole excitations in deformed nuclei at excitation energies near 2.5 MeV. The transition energies and the enhanced $B(E1)\uparrow$ strengths of $3\text{-}5\cdot10^{-3}$ e^2fm^2 may suggest an interpretation in terms of the predicted new type of collective electric dipole excitations in deformed nuclei due to reflection asymmetric shapes like octupole deformations and/or cluster configurations. Furthermore, all these states systematically exhibit decay branching ratios $R_{exp} = B(1^- \rightarrow 2_1^+)/B(1^- \rightarrow 0_1^+)$, which hint at I<-mixing. Another very tempting interpretation of these strong $E1$ excitations is the explanation as two phonon excitations due to the coupling of octupole ($J = 3^-, K = 1$) and quadrupole-γ-vibrations ($J = 2^+, K = 2$). The results can be explained in the framework of the sdf-IBA model and the Dynamic Collective Model describing octupole vibrations and their coupling to quadrupole vibrations in deformed nuclei. First results for a spherical, odd mass nucleus are presented. In the even N=82 isotones strong $E1$ excitations are known which can be interpreted as transitions to the $J^\pi = 1^-$ members of $2^+ \otimes 3^-$ multiplets. The coupling of an additional neutron to these two-phonon excitations has been studied in ^{143}Nd. In this nucleus recent experiments succeeded in the first identification of dipole excitations to a $2^+ \otimes 3^- \otimes$ particle multiplet.

*Supported by the Deutsche Forschungsgemeinschaft under contract Kn 154-21 and SFB 201 Mainz

I. Introduction

The use ofelectromagnetic probes sucli as real photons (y-quanta) or virtual photons (inelastic electron scattering) in nuclear structure research offers some attractive features and fundamental advantages. The excitation mechanism is well known and leads to tlie population of states with *low* spins[1]. In real photon absorption the transfer of momentum q is equal to the excitation energy ω (in units of $\hbar = c = 1$); it is low and *fixed.* Therefore, mainly electric dipole excitations (E1) occur, and to much less extent electric quadrupole (E2) or magnetic dipole ($M1$) excitations are induced. The use of linearly polarized photons or the measurement of particle polarizations enable to distinguish between electric and magnetic excitations[2]. On the other hand, *in* electron scattering experiments (exchange of virtual photons) the transfer of momentum q can be varied independently of the excitation energy *w* by changing the kinematics (incident electron momentum k_0 and/or scattering angle Θ_e)[1]. Therefore, in principle, different multipoles can be excited rather specifically. Tlie measured form factors provide unique information on transition densities[1,3]. IIowever, at excitation energies above the particle thresholds the full information is only accessible when performing $(e, e'X)$-coincidence experiments [3,4]. Unfortunately, these experiments had to wait for the construction of modern high duty cycle electron accelerators. Furthermore, these machiiies allow to produce monochromatic tagged photons witli reasonable Auxes and to perform single arm counting experiments at high counting rates since the pile-up problem is drastically reduced as compared to experiments using pulsed accelerators. The availability of tlie new CW electron accelerators together witli improved particle detection techniques led to a new generation of photonuclear experiments.

In the light of the new CW 30 MeV race track microtron under construction at the University of São Paulo I want to restrict myself in this report to the discussion of typical *low* energy pliotonuclear reaction studies. The design energy of this machine (30 MeV) is too low to achieve in $(e, e'X)$-experiments the momentum transfers q needed to excite multipoles higher than L = 1 (dipole). Therefore, the favoured application of this accelerator mainly should be devoted to experiments with real photons (y-quanta). Two topics out of this field are emphasized in this report which make use of the high spin selectivity of electromagnetic probes and which document the progress achieved in the last years due to the advent of CW electron accelerators and sophisticated detector and spectrometer set-ups:

- Low energy photofission: Fragment angular distributions near the fission barrier
- Low energy photon scattering: Magnetic and electric dipole excitations in heavy nuclei

Both classes of experiments have the common feature to investigate collective excitations of nuclei at large deformations. Measurements of fragment angular distributions at excitation energies near the barrier enable to pin down the spectrum of transition states on top of the fission barrier and, hence, to study low-lying, collective excitations at ***high*** deformations (more than twice the groundstate deformation)[5,6]. By measuring simultaneously fission fragment mass distributions the influence of the excitation and of the specific nuclear structure of tlie excited state on the fission path can be studied for the first time[7–9]. This allows to investigate tlie coupling of tlie socalled Bohr fission channels[10] to the diverse fission modes ("Brosa modes")[11] resulting in different fission fragment mass distributions .

Low energy photon scattering off bound states, nuclear resonance fluorescence (NRF), represents a highly selective and sensitive tool to investigate low-lying more or less collective dipole excitations in lieavy nuclei. Tlie discovery of a new class of enhanced magnetic excitations in lieavy deformed nuclei in high resolution electron scattering experiments by Richter and coworkers[12] initiated numerous electron and photon scattering experiments[13–16] to study tlie fragmentation and systematics of this mode often referred to as "Scissors *Mode*". On the other hand, these NRF-experiments also provided evidence for enlianced, low-lying electric dipole excitations in deformed nuclei[17–19]. The structure of the corresponding $J^\pi = 1^-$ states are discussed in terms different collective excitation modes or two phonon excitations. For odd mass nuclei there are interestings topics

like the search for the first detection of the *"Scissors Mode"*[20] or the investigation of dipole excitations to two-phonon-particle multiplets in spherical nuclei near closed shells[21].

Both kinds of experiments discussed in this report make great demands upon the required accelerators and detector systems. (e,$e'f$)-coincidence and tagged photon experiments are only feasible at high duty cycle electron accelerators. The corresponding experiments[4 22] reported were performed at the second stage of the Mainz microtron[23] and at the superconductive microtron in Urbana[8]. The photofission experiments using linearly polarized bremsstrahlung[9,24] ask for high intensity machines in order to produce a reasonable flux of polarized photons. These experiments were performed at the Giessen Linac[25], which is now shut down. However, such experiments are highly desirable to be carried out using polarized *monochromatic* tagged photons. For the simultaneous measurement of both fission fragment angular distributions and mass distributions, 4π-arrangements of fragment detectors with electronical read out are needed[26]. Different set-ups mainly of parallel plate avalanche counters (PPAC's)[27] or multiwire proportional chambers (MWPC's)[28] have been recently used.

The photon scattering experiments require a high intensity, CW bremsstrahlung beam to succeed in getting a high detrction sensitivity even when using a small amount of necessarily enriched target material (1-3 g of total mass). The high duty cycle is obligatory to operate the γ-spectrometers at high counting rates without pile-up. High resolution Ge-y-spectrometers of good efficiency have to be used. For parity assignments Ge-Cornpton polarimeters are needed[29,30]. The experiments reported were performed at the photon scattering facility[15,31] installed at the high current Stuttgart Dynamitron (E_{max}= 4.3 MeV; I^{-}_{max}= 4 mA)

II. Low energy photofission: fragment angular distributions

II.1 The transition state concept

The measurement of fission fragment angular distributions represents an important tool to investigate the properties of the fission barriers. At energies near the barrier the fragment angular distributions can be explained within A.Bohr's fission channel concept[10]. At these excitation energies most of the available energy has been expended into deformation energy, when the fissioning nucleus reaches the saddle point. Therefore, the system should be thermodynamically rather "cold" at this highly deformed configuration and exhibits a discrete spectrum of low-lying collective excitations similar to that at the groundstate deformation. Within Bohr's hypothesis it is assumed that the near barrier fission takes place through these discrete, so called transition states. With the assumptions that the fission process proceeds along the symmetry axis of the deformed nucleus and that the projection K of the spin J of the excited state onto the symmetry axis is conserved during the path from the saddle to the scission point, the fragment angular distributions are determined by the quantum numbers J and K of the transition states involved.

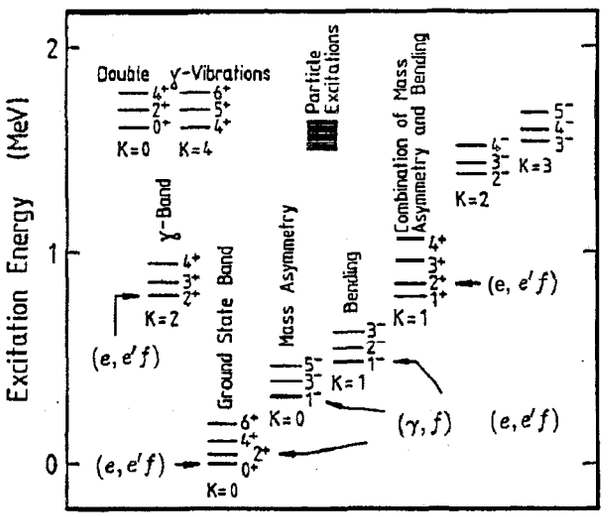

Figure 1: The schematic presentation of the spectrum of transition states in the case of even-even actinide nuclei[5]. Transition states which have been investigated so far by virtual (e,e'f) and real (y, f) photon experiments are indicated.

Fig.1 shows schematically the expected spectrum of transition states for an even-even nucleus, which represents the most favourable case, since the collective bands lie well below the intrinsic, single particle excitations (due to the pairing gap). The relative positions of

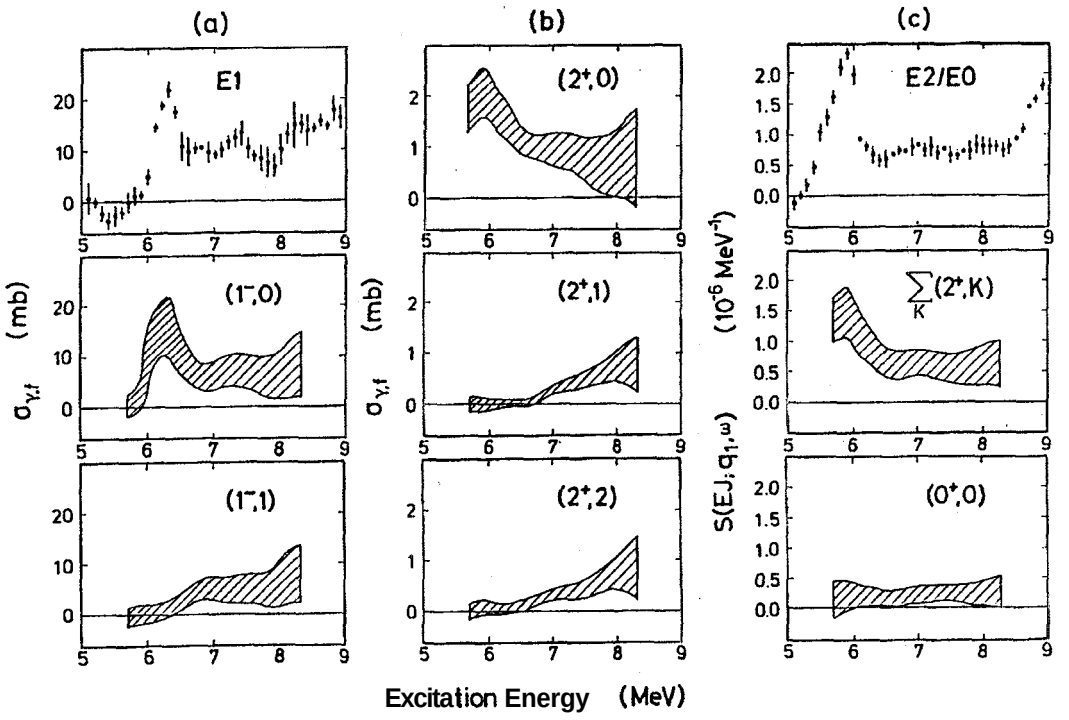

Figure 2: Separated fission cross sections for partial fission channels (J^π,K) of ^{238}U: (a) total $E1$ cross section and its separation into the (1–,O) and (1–,1) fission channels, (b) cross sections for the separated $(2^+,0)$, $(2^+,1)$, and $(2^+,2)$ fission channels, and (c) total $E2/E0$ strength distribution (from multipole decomposition), measured at $q_1 = 0.20$ fm^{-1} and its separation into the sum of all $(2^+,K)$ fission channels and the $(0^+,0)$ fission channel (from Ref. [22]).

the collective bands (groundstate rotational band, octupole bands, y-vibration etc.) strongly depend on the nuclear shapes at the saddle. Therefore, fragment angular distributions, which allow to identify specific transition states, reveal a direct information on the nuclear shape at the extreme deformation of the saddle point.

11.2 F'ragment angular distributions in (e,e′f)-coincidence experiments

Using real photons to excite an even-even nucleus and with the reasonable restriction to $E1$ and E2 excitations five transition states ($J^\pi = 1-, K = 0,1$ and $J^\pi = 2^+, K = 0,1,2$) can contribute to the nuclear fission process. The photofission fragment angular distribution can be parametrized as[5,6]

$$W(\Theta) = a + b\cdot\sin^2\Theta + c\cdot\sin^2(2\Theta)\,. \quad (1)$$

The coefficients a and b arise from both dipole and quadrupole contributions, whereas c comes entirely from quadrupole fission. In general, the 5 above mentioned fission channels cannot be disentangled by measuring the three coefficients a, *b*, c. Therefore, the analysis of photofission angular distributions has to be restricted to the discussion of the three channels assumed to be the lowest in excitation energy ($J^\pi = 1^-$, $K = 0,1$ and $J^\pi = 2^+$, $K = 0$). On the other hand, the possible q-variation in exclusive (e,e′f)-coincidence experiments allows to disentangle 6 transition states in even-even nuclei ($(J^\pi,K) = (0^+,0), (1^-,0), (1^-,1), (2^+,0), (2^+,1)$, and $(2^+,2)$) by measuring at at least two different momentum transfers. This has been recently demonstrated by (e,e′f)-coincidence experiments [4,22] performed at the 185 MeV stage of the Mainz microtron.

The results are plotted in Fig.2: for $E1$ and E2 the deduced partial strength distributions $s(J^\pi,K;w)$ are converted into the respective partial photofission cross sections $\sigma_{\gamma,f}(J^\pi,K;w)$. Since for $E0$ no photofission cross section exists, the respective strength distribution is plotted. From the increase of the partial fission cross sections the effective barriers of the respective fission channels (J^π,K) can be estimated[4,22].

The fission barriers of the already known (1–,O), $(1^-,1)$, and $(2^+,0)$ channels are in reasonable agreement with the results o-' previous (γ,f)[32–34] and inclusive (e, f) experiments[35]. Also for the $(0^+,0)$ channel the data from direct reaction studies[36] are not in contradiction with the barrier height in the present experiment which can be estimated only rather roughly. Microscopic QRPA calculations[37] and recent $(a,\alpha' f)$ experiments[38] corroborate the rather negligible $E0$ cross section in the excitation energy region up to 8 MeV. Furthermore, for the first time, for the $(2^+,1)$ and $(2^+,2)$ cliannels an estimate of the effective fission barriers can be given[4,22].

Comparing the results for ^{238}U with the theoretically expected spectrum of low-lying collective transition states of an even-even nucleus (see Fig.1) a surprisingly good agreement can be found. The lowest $(0^+,0)$ and $(2^+,0)$ states occur within the rotational groundstate band which is reasonable to be the lowest band in ercitation energy. The 1^- transition states are found at higher excitation energies as band heads of the mass asymmetric octupole band ($K = 0$) and the bending octupole band ($K = 1$), respectively. The $(2^+,2)$ transition state can be ascribed to the head of the y-vibrational band whereas the first $(2^+,1)$ state is found within an octupole band resulting from a combination of mass asymmetry and bending, both at slightly higher excitation energies.

II.3 Mass dependence of photofission fragment angular distributions

As already discussed the fragment angular distribution in photofission of even-even nuclei is given by equ.(1). The coefficients a and b contain both, dipole and quadrupole contributions; whereas c comes entirely from quadrupole fission. Tabulations of the coefficients a, b, cfor the different fission channels J,K can be found in the literature[5,6]. The analysis of photofission angular distributions has to be restricted to the three channels lowest in excitation energy ($J^\pi = 1^-$, $K = 0,1$ and $J^\pi = 2^+$, $K = 0$). For pure dipole fission ($J = 1$) or the excitation of the lowest $K = 0$ states the quantities b/a and c/b are related to the partial cross sections $\sigma_{\gamma,f}(J^\pi,K)$:

$$b/a = \frac{\sigma_{\gamma,f}\ (J^\pi = 1^-, K = 0)}{\sigma_{\gamma,f}\ (J^\pi = 1^-, K = 1)} - 1/2 \qquad c/b = \frac{5}{4} \cdot \frac{\sigma_{\gamma,f}\ (J^\pi = 2^+, K = 0)}{\sigma_{\gamma,f}\ (J^\pi = 1^-, K = 0)} \qquad (2)$$

In the case of sufficiently low photon energies, where only states with $K = 0$ should be excited, the ratio c/b directly measures the relative quadrupole contribution. The systematics of the ratio of dipole to quadrupole photofission has been studied already in the pioneering work by Rabotnov and coworkers[39]. This quantity c/b is very sensitive to the relative heights of the lowest 1^- and 2^+ transition states. In the picture of the double humped fission barrier with a mass asymmetric outer barrier the dipole to quadrupole photofission provides direct information on the relative heights of the inner and outer barriers as pointed out by Vandenbosch[40].

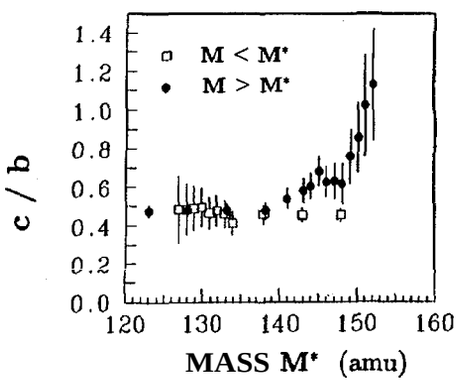

Figure 3: Relative quadrupole contribution c/b as a function of a variable mass M* which divides the mass distribution into mass regions M < M* and M > M*, respectively. The data were observed for ^{236}U(γ, f) at a bremsstrahlung endpoint energy of $E_{BS} \approx 5.7$ MeV[7].

In a recent experiment[7] for the first time the fission fragment angular and mass distributions have been measured simultaneously for the reaction $^{236}U(\gamma, f)$, using the 4π-arrangement of position sensitive PPAC's[28]. The aim of this experiment was to search for a possible correlation between the multipolarity of the excitation (spin and K-value of the transition states involved) and the fragment mass asymmetry. The obtained results clearly establish a correlation between the fragment mass asymmetry and and the angular distributions given by the quantum numbers of the transition states involved. In Fig. 3 the ratio c/b is plotted as a function of a variable mass M^* which divides the mass distributions into masses $M \leq M^*$ and $M \geq M^*$. For $M \leq M^*$ the ratio c/b is almost constant as a function of M^*. However, for $M \geq M^*$ a distinct increase of c/b can be stated, starting at around $M^* \approx 140$. This observed increase for a "far asymmetric" mass split ($M^* \geq 140$) gives rise to the assumption that a quadrupole photoabsorption at excitation energies near the barrier leads to a stronger coupling to the standard II fission channel within Brosa's multi exit fission channel model[11].

11.4 Photofission using linearly polarized photons

The 1^+ transition state within a $K = 1$ octupole band (see Fig.1), corresponding to a $M1$ excitation, cannot be investigated in $(e, e'f)$-coincidence experiments since transverse excitations can only be studied at backward scattering angles, where, unfortunately, the cross sections are very small. An alternative represents the use of linearly polarized photons. Then the fragment angular distribution for dipole fission of an even-even nucleus is given by

$$W(\Theta) = a + b \cdot \sin^2\Theta \cdot \{1 + \omega \cdot P_\gamma \cdot \cos(2 \cdot \Phi_f)\} \cdot \quad (3)$$

Here Φ_f is tlie azimuthal angle between the polarization plane, defined by the electric field vector $\vec{E}$ and the beam direction, and the reaction plane. The factor w is -1 for magnetic and $+1$ for electric excitations, respectively. The experimental asymmetry ε, the product of the degree of polarization P_γ and the analyzing power C is given by

$$\varepsilon(\Theta) = P_\gamma \cdot \Sigma(\Theta) = \frac{W(\Theta, \Phi_f = \pi/2) - W(\Theta, \Phi_f = 0)}{W(\Theta, \Phi_f = \pi/2) + W(\Theta, \Phi_f = 0)} \cdot \quad (4)$$

Multipole	K	b/a	C $(\Theta = \pi/2)$
E1	0	$+\infty$	–1
E1	1	$-1/2$	+1
M1	1	$-1/2$	-1

'Eable 1.: Angular correlation coefficients and analyzing powers for dipole photofission using polarized photons[6,24].

The analyzing power is maximal under $\Theta = \pi/2$ and changes its sign for electric and magnetic excitations (see Table 1). Therefore, the measurement of ε enables model independent parity assignments. In the case of dipole excitations C is simply given by

$$\Sigma(\Theta = \pi/2) = -\omega \cdot \frac{b/a}{b/a + 1} \cdot \quad (5)$$

The full formalism is described elsewhere[6,24].

The experiments[9] have been performed at the Giessen facility for polarized off-axis bremsstrahlung[25]. The average degree of polarization P_γ measured via the photodisintegration of deuterium amounted to about 15-20%. The fragments were detected by the Giessen 4π-arrangement of position sensitive PPAC's[28] enabling the simultaneous measurements of both fragment angular and mass distributions. The isotope ^{232}Th has been chosen, since Th-nuclei are known to have a mass asymmetric outer barrier with

negative and positive parity bands[41] and, furthermore, only negligible E2 contributions have been observed in photofission work using unpolarized photons[39].

Three mezsurements had been carried out on ^{232}Th at bremstrahlung endpoint energies of E_{BS}= 12.0, 11.0, and 10.5 Me'? with polarized off-axis bremsstrahlung. In Fig.4 the results for the ratio b/a and ε (O = $\pi/2$) are plotted as a function of the mass parameter M*, already introduced. A value of M*= 117 means that fragment masses of the whole mass distribution were considered in the analysis. With an increasing value of M* only fission events with a heavy mass $M_h \geq$ M* have been taken into account. In all three measurements the ratio b/a increases for more and more asymmetric fission events (M* $\geq$ 140). Therefore, it is of interest to consider the b/a systematics in the framework of Brosa's "multi exit channel" model[11]. The mass asymmetric so called star dard II mode contributes' exclusively for values M* $\geq$ 145. Neglecting contributions of the mass symmetric "superlong" mode the measured angular distribution at M* = 117 is determined by a weighted superposition of the standard I and standard II intrinsic angular distributions. The corresponding weights of both modes could be deduced from the measured fission fragment mass distributions. With these input data it was possible to calculate b/a as a function of M*. The dashed lines in Fig.4 represent the results. The general trend of the measured data could be qualitatively reproduced.

The ratio b/a also measures directly the ratio of the partial cross sections for fission through the K = 0 and K = 1 transition states (b/a = $\{\sigma_{\gamma,f}(1^-,0) / \sigma_{\gamma,f}(1^-,1)) - 1/2$). An increasing value of b/a for far asymmetric fission events points to a lowered ($J^\pi = 1^-$, K = 0) barrier relative to the ($J^\pi = 1^-$, K = 1) barrier. This seems to be understandable since the collective (1^-, 0) excitation belongs to a pear like deformation and the outer barrier is known from theoretical calculations to be energetically reduced when taking into account reflection asymmetric deformations of the nucleus[36]. Without discriminating between different fragment mass regions (M* = 117) the asymmetries ε (O = $\pi/2$) showed negative values of the order of $\approx -10\%$. Within the error bars these values are in agreement with the assumption that only *electric* dipole excitations take place. Furthermore, the measured data are in agreement with an former experiment also performed at the Giessen off-axis bremsstrahlung facility, however with modest angular resolution and *without* mass separation[24]

The mass dependence of E (O = $\pi/2$) changes from higher to lower bremsstrahlung endpoint energies. If we asssume that only dipole excitations contribute and that the relative contributions of the $(1^+,1)$ and $(1^-,1)$ fission channels will not depend on fragment masses, the asymmetry ε (O = $\pi/2$) can be calculated from the measured b/a values[24]. The dashed areas in the right part of Fig. 4 shows the results. At least for the lowest energy E_{BS}= 10.5 MeV a discrepancy between the the calculated and measured azimuthal asymmetry can be stated. A possible enhanced *magnetic* dipole contribution would contribute with a negative-value and would increase the asymmetry to higher absolute values. Therefore, the observed decreased absolute value must be regarded as a hint for quadrupole excitations which become important. Only the $(2^+,2)$ channel contributes with a positive sign at $\Theta = \pi/2$. The corresponding K = 2 transition state is the head of the y-vibrational band, which seems to be lowered at the outer barrier in the case of a far asymmetric mass split.

In the case of ^{236}U($\vec{\gamma}$, f) one measurement at E_{BS}= 9.0 MeV was carried out[9]. This endpoint energy was still to high in order to observe strong quadrupole contributions. The measured values of the azimuthal asymmetry without mass discrimination amounted to about -6%, that means half the value observed in the Th measurements. However, that is what is expected from the fission barrier structure of ^{236}U (inner and outer barrier are nearly of the same heights), leading to reduced b/a ratios and hence to lower asymmetries E. The b/a ratio was observed to increase for far asymmetric fission as it was seen in the Th measurements. The value of the azimuthal asymmetry remained nearly constant within the statistical errors as a function of M*.

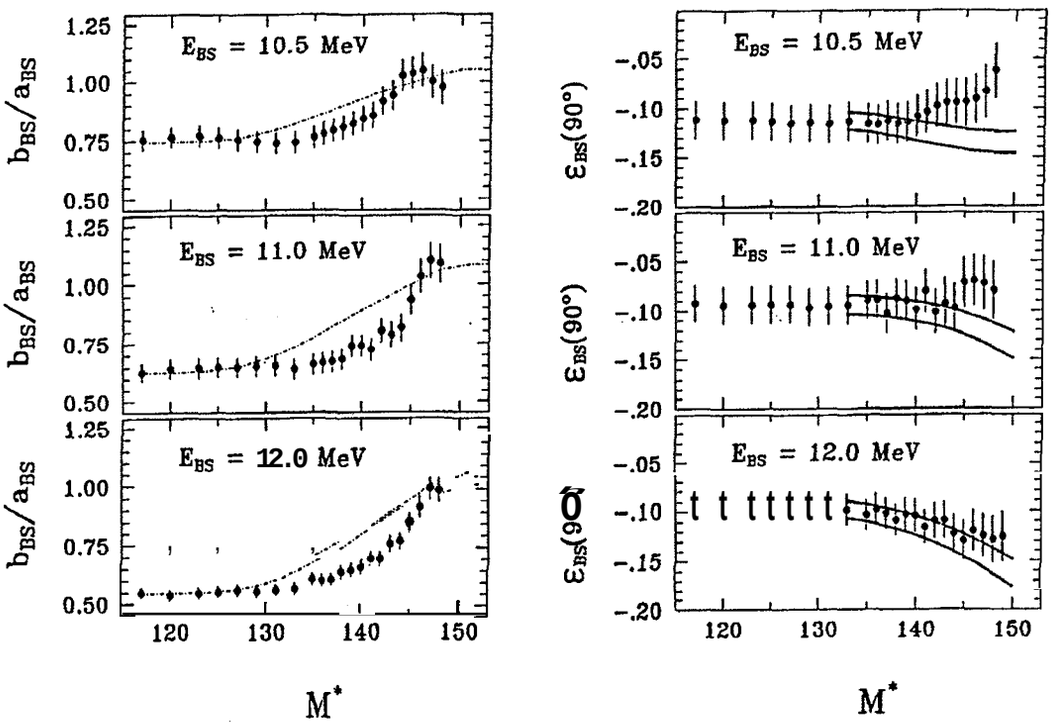

Figure 4: Left Part: The dependence of b_{BS} / a_{BS} on M* and E_{BS} deduced from experiments on ^{232}Th.
Right part: The dependence of $\epsilon_{BS}(\theta = 90°)$ on M^* and E_{BS} deduced from experiments on ^{232}Th (note that the data points for different values of M^* are not statistically independent from each other). The dashed iines are the limitations of the expected values $\epsilon_{BS}(\theta = 90°)$ as described in the text (from Ref.[9]).

11.5 Second chance photofission using tagged photons

First measurements of the angular and mass distributions of fragments from photofission using monochro*matic* tagged photons have been performed by a Giessen-Urbana collaboration[8] at the tagged photon facility of the University of Illinois. The fragments were detected by the Giessen 4π-PPAC arrangement[28]. Unfortunately, the photofission cross section near the barrier is very small (a few mb), so a Iarge amount of beam time is required for measurements of angular distributions, which need excellent statistics. In the energy range of the second–chance fission threshold, B_{nf}, the cross sections are significantly higher. Therefore, one motivation for this experiment was to take advantage of the higher cross section in this region and investigate the angular distributions of fission fragments from ^{238}U after neutron evaporation in order to obtain information on the low-lying transition states in ^{237}U. It is also worth mentioning that target nuclei that are unstable become accessible by studying fission at the second chance fission threshold (^{237}U in the case of this experiment).

The surprising novel result of the experiments was the first observation of anisotropic angular distributions in the energy range of the second chance fission threshold ($\approx$ 12 MeV in ^{238}U). At these energies electric dipole excitations dominate and E2 contributions can be neglected. A combined analysis of the present (γ, nf)-data and results of recent (e, e'n f)-experiments[4] and a comparison with previous ^{239}Pu(γ, f)-data[42] (^{239}Pu has the same groundstate spin of $1/2^+$ as ^{237}U) enabled a consistent spin and K-number assignment to two low-lying transition states in ^{237}U (E, $\approx$ 11.3 MeV: $J'' = 3/2^-$, $K = 3/2$; E, $\approx$ 12.6 MeV: $J'' = 5/2^+$, $K = 5/2$). Furthermore, a clear relationship between the anisotropies and the fragment mass asymmetry has also been established. This correlation, together with the energy dependence of the angular distribution parameters, points to a possible interpretation of the results in terms of a recent theoretical model incorporating multiple exit channels in fission[11].

11.6 Contributions of **odd** harmonics to photofission **fragment** angular distributions

The formalism to describe fission fragment angular distributions which was introduced so far does not distinguish between the emission directions of light and heavy fragments and the expected fission fragment angular distributions show a symmetry with respect to $\Theta = \pi/2$. If one can distinguish experimentally between iight and heavy fragments, the investigation of the angular correlation $q \cdot p_l$ (where q is the momentum of the photon and p_l is the momentum of the light fragment) allows to study a possible appearance of odd harmonics in the fragment angular distributions. This is expected because of interference effects between transition states of spposite parity and was already discussed by Hittmair, Wheeler and Flambaum[43–45]. Transition states with different values of the quantum number K do not interfere since they correspond to different internal states of the nucleus. If one takes into consideration dipole and quadrupole excitations and with the restriction to photofission induced by unpolarized photons the polar angular distribution has to be extended by an additional term $\propto \cos(\Theta)$[45]. It takes the form

$$W(\Theta) = P + R \cdot \cos(\Theta) \,, \qquad (6)$$

with the abbreviations

$$P = a + b \cdot \sin^2(\Theta) + c \cdot \sin^2(2\Theta) \qquad (7)$$

$$R = f + g \cdot \sin^2(\Theta) \,. \qquad (8)$$

The ratio R/P measures the relative contribution of odd harmonics in the angular distributions.

The asymmetry in fission fragment angular distributions with respect to $\Theta = \pi/2$ was explored by Baumann et al.[46] for neutron induced fission of ^{230,232}Th. A slight but significant asymmetry was observed in the case of ^{230}Th(n,f). In a quite recent experiment Steiper et al.[9] tried to detect this effect in the case of the ^{236}U(γ,f) process at bremsstrahlung endpoint energies between 5.5 MeV and 6.25 MeV where considerable contributions of the $((J^{\pi}K) = 2^+, 0)$ transition are involved in the fission process[7]. At photon energies $E_\gamma \approx 5$ MeV the ratio R/P (see equations 7 and 8) is assumed to be considerable because the amplitudes A_L of fission induced by a photon of multipolarity $E1$ or E2 are of the same strength $(A_{E1} \approx A_{E2})$[45]. In contrast to neutron induced fission no intensive monochromatic sources exist for photons which allow to perform precise measurements of photofission angular distributions at such low energies. The study of P-odd asymmetries by nonmonochromatic photon beams causes a drastic reduction of the measurable quantity R/P.

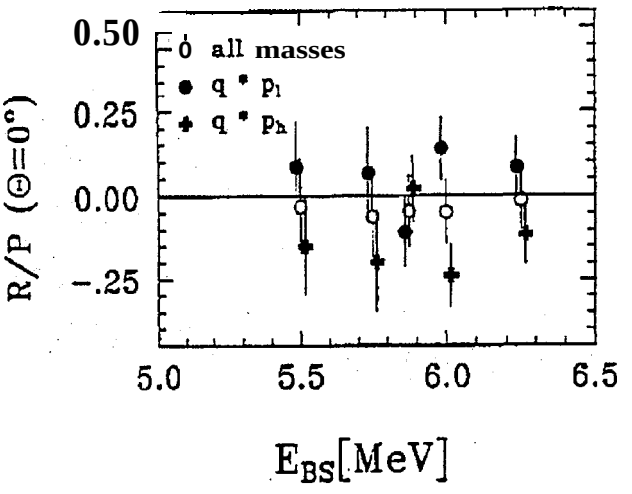

Figure 5: The ratio $R/P(\theta = 0°)$, which measures the relative contributions of odd harmonics to the angular distributions, as a function of E_{BS}. Open symbols illustrate the results without distinguishing between fragment masses; the other data points represent the angular distributions of light $(q \cdot p_l)$ or heavy $(q \cdot p_h)$ fragments (see text) (from Ref.[9]).

The measured angular distributions for light (heavy) fragments were analyzed to investigate the angular correlation $q \,.\, p_l$ $(q \,.\, p_h)$ and to deduce the ratio R/P (O, E_{BS}). The data points in Fig. 5 represent the experimental values of R/P $(O = 0°, E_{BS}) = f/a$ (E_{BS}). For a comparison, f/a values of angular distributions obtained from fission fragments of the whole mass distribution were plotted. Within the error bars the ratio f/a vanishes if one does not distinguish between heavy and light fragment masses; in such cases the data points show a small negative value. This could be a hint for a small misalignment of the orientation of the fission detector relative to the direction of the photon beam. Because the angular distributions of heavy and light fragments are correlated, nonvanishing ampli-

tudes of odd harmonics should have opposite signes but similar absolute values. The data points representing the angular correlations $q \cdot p_l$ and $q \cdot p_h$ showed this expected behaviour when taking into account a possible misalignement of the experimental setup. Nevertheless the size of the error bars made it impossible to obtain clear and definite evidences for the existence of odd harmonics. A χ^2 test carried out by fitting the data according equation 6 with and without terms $\propto \cos(\Theta)$ showed that only the data obtained at $E_{BS} = 6.0$ MeV can be influenced by the contribution of odd harmonics in the angular distributions (with terms $\propto \cos(\Theta)$: $\chi_l^2 = 1.074$, $\chi_h^2 = 0.888$; without terms $\propto \cos(\Theta)$: $\chi_l^2 = 1.923$, $\chi_h^2 = 1.639$). Figure 6 explicitly shows the measured angular distributions and the adapted parameterization curves. In Ref. [45] it was also mentioned that R/P might depend on the particular fragment mass regions if the fission amplitudes A_L in different fission channels are different. Basically, the detector arrangement used[28] allowed the measurements of such dependences but the limited statistics at low photon energies made it impossible to deduce unambigous information. Obviously, higher statistics combined with the use of monochromatic photons would give a more clear result.

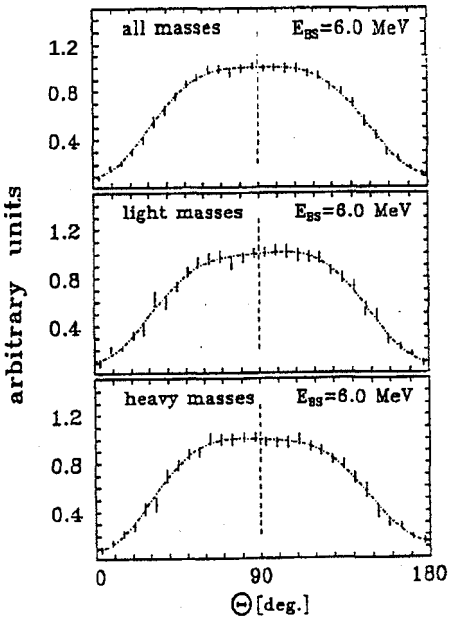

Figure 6: The fragment angular distributions measured in photofission of ^{236}U induced by a bremsstrahlung spectrum with an endpoint energy of 6.0 MeV. The solid lines are the results of fits according to equation (6) (from Ref.[9]).

III. Low energy photon scattering: dipole excitations in heavy nuclei

III.1 Motivation

Over the last years, an increased interest has been shown in the study of low-lying, enhanced dipole excitations in deformed nuclei both of magnetic and electric multipolarity. There have been hints from experimental work and theoretical calculations for the occurrence of enhanced electric dipole transitions in deformed, heavy nuclei due to reflection asymmetric shapes[47,48]. Very recently Butler and Nazarewicz[48] discussed and explained intrinsic electric dipole moments in nuclei of the Ra-Th and Ba-Sm region deduced from studies of alternating parity bands with enhanced $E1$ and E3 transitions and parity doublets. As discussed by Iachello[49] specifialy for the deformed rare earth nucleus ^{150}Nd, rather collective $E1$ *groundstate* transitions are expected from states near 3 MeV excitation energy due to α-cluster configurations and/or octupole deformations. On the other hand, it is well known that in the same excitation energy range around 3 MeV strong orbital magnetic dipole excitations occur in deformed nuclei, often referred to as the "Scissors *Mode*". This magnetic mode was discovered in high resolution electron scattering experiments by Richter and coworkers in 1984[12]. Meanwhile it has been investigated in numerous electron and photon scattering experiments[13–16] These studies showed that the $M1$ strength can be rather fragmented. Therefore, parity determinations are imperative for photon scattering experiments when searching for the above mentioned new electric dipole modes in the same energy region as the orbital magnetic dipole excitations.

III.2 Experimental techniques

III.2.1 The nuclear resonance fluorescence method

Nuclear resonance fluorescence (NRF) experiments (photon scattering off bound states) represent an outstanding tool to investigate these low-lying dipole excitations and to provide detailed spectroscopic informations. The low transfer of momentum q of real pho-

tons makes photon scattering highly selective in exciting low spin states. In particular, only E1, $M1$, and, to a much lesser extent, E2 transitions are induced. In addition, modern y-spectroscopy offers highly efficient Ge-detectors with an excellent energy resolution, with which the NRF method can achieve a high sensitivity. This sensitivity is essential for detailed studies of the fragmentation of the strengths of specific collective modes. Furthermore, the use of continuous bremsstrahlung radiation enables all states with sufficient ground state decay widths to be excited simultaneously. There are no limitations as in experiments using monoenergetic photons from capture reactions, where a chance overlap of the incident photon energy and the energy of the excited nuclear state is necessary.

The fundamental advantage of the photon scattering technique is the well-understood mechanism of excitation *and* deexcitation via the electromagnetic interaction. Therefore, the following quantities can be extracted in a completely model independent way[25]

- the excitation energies.
- the ratio Γ_0^2/Γ, (Γ_0 and Γ: ground state and total decay widths, respectively).
- the spins of the excited states.
- the branching ratios for the decay to excited states.
- the parities of the excited states.

So far, in most of the previous systematic photon scattering experiments, parity assignments came from a comparison with electron scattering form factors[50] or by applying the Alaga rules[51]. Within their validity the measured decay branching ratios to the first excited 2^+ state and to the 0^+ ground state ($R_{exp} = B(1 \rightarrow 2_1^+) / B(1 \rightarrow 0_1^+)$) enable in even-even deformed nuclei to determine the K-quantum numbers of the excited states. Negative parities can be assigned to $K = 0$ levels, whereas for $K = 1$ states either negative or positive parities are possible. Parities can be determined model independently in photon scattering experiments by measuring the linear polarization of the scattered photons using Compton polarimeters. The parity information is obtained from the measured azimuthal asymmetry ε

$$\varepsilon = \frac{N_\perp - N_\parallel}{N_\perp + N_\parallel} = P_\gamma \cdot Q \,, \qquad (9)$$

where $N_\perp$ and $N_\parallel$ represent the rates of Compton scattered events perpendicular and parallel to the NRF scattering plane defined by the directions of the photon beam and the scattered photons, respectively. The asymmetry ε is given by the product of the polarization sensitivity Q of the polarimeter and the degree of polarization P_γ of the scattered photons. At a scattering angle of $\Theta = 90^0$ to the beam axis the polarization P_γ amounts to -1 or $+1$ for pure $E1$ and $M1$ excitations, respectively (0-1-0 spin sequences). Therefore, obviously the sign of the asymmetry ε determines the parity.

III.2.2 The Stuttgart photon scattering facility

The experiments have been performed at the bremsstrahlung facility installed at the Stuttgart Dynamitron accelerator (E_0 = 4.3 MeV; $I^-_{typical} \approx$ 0.8 mA (CW)). In total, mostly three detector set-ups were operated simultaneously at the photon beam:

- a 3 Ge-detector arrangement to measure angular distributions and scattering cross sections in NRF experiments (without polarization sensitivity) as described in[31].
- a five crystal Compton polarimeter with a central Ge-detector and four peripheral Ge or Ge(Li)-detectors located below the scattering target[29].
- a sectored true coaxial Ge(HP)-polarimeter installed in a horizontal scattering plane at a scattering angle $\Theta = 95^0$. The characteristics of this new polarimeter are described in more detail in the following section.

The scattering targets consisted of cylindrical discs of enriched isotopes with diameters of 2 cm and masses

of ≈ 3 - 10g. Plates of aluminum sandwiched the targets. The lifetimes and decay properties of three ^{27}Al levels below 4 MeV are precisely known[52]. Therefore, the numbers of photons resonantly scattered off these levels were used for the absolute calibration of the incoming photon flux. Furthermore, the 2.981 MeV line produced by resonant scattering off ^{27}Al is known to be effectively unpolarized ($P_\gamma = 1.5\%$) and served as online test of the performances of the polarimeters. The photon scattering technique, the experimental setups and procedure are described in detail in preceding papers[15,31].

III.2.3 A sectored Germanium single crystal compton polarimeter

This new polarimeter consists of a true coaxial p-type Ge(HP) crystal with its outer n-type contact splitted into four electrically insulated surfaces resulting in four electrically separated sectors. The outer surface of each sector and the inner p-type core have electric contacts connected to separated preamplifiers. The signal from the central core directly provides the total energy of the incident photon, whereas the signals from the sectors are used to define different coincidence conditions, permitting to use the sectored detector as a Compton polarimeter. The dimensions of the crystal and the coincidente configurations are shown in Fig. 7. In spite of the lower polarization sensitivity Q of the single crystal polarimeter as compared to that of a five detector set-up the high coincidence efficiency ϵ_c makes the sectored polarimeter a competitive instrument. Furthermore, this type of polarimeter needs no energy summation to determine the total energy of the incident photons. This feature is of particular advantage in NRF experiments using continuous bremsstrahlung where an excellent energy resolution and long time stability are of crucial importance.

The characteristics of the fourfold sectored Ge(HP)-Compton polarimeter are summarized in Table 2. The polarization sensitivity of the device has been determined in the energy range up to 4.4 MeV studying $(p,p'\gamma)$-reactions on ^{12}C, ^{24}Mg, ^{28}Si and ^{56}Fe at the Cologne Tandem facility and the Stuttgart Dynamitron. The polarization sensitivity Q amounts to ≈ 20% at 0.5 MeV and remains ≈ 9.5% at 4.4 MeV[30]. The overall detection sensitivity of the polarimeter will be considerably increased in the near future by improving its response function using a BGO anti-Compton shield[53].

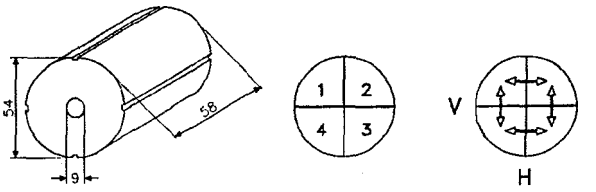

Figure 7: Layout of the fourfold sectored Compton polarimeter (dimensions in *mm*), the numbering of the four sectors, and the coincidence requirements defining horizontal (H) and vertical (V) Compton events (see refs.[16,30]).

111.3 Results for M1 excitations in even-even nuclei

The first report on a new *magnetic* dipole mode in deformed nuclei by Richter and coworkers[12] in 1984 stimulated a huge number of both experimental and theoretical work (for an overview of references see[13,14]). This predominantly orbital excitation seems to be a rather general phenomenon. Today it is established by numerous systematic electron and photon scattering experiments[13–16], not only in deformed nuclei of the rare earth mass region, but it has been observed in actinide isotopes[54,55] as well. Intuitive terms like "*Scissors Mode*", "*Nuclear Wobble*", and "*Giant Angle Dipole*" have been attributed to these low lying isovector $M1$ excitations which originally have been discussed in the framework of the Two Rotor Model[56] and the IBM-2 version of the Interacting Boson Model[57]. On the other hand, to explain the underlying microscopic structure of these low-lying 1^+ - states several groups performed different quasiparticle random phase approximation (QRPA) calculations[58–64].

The measurements of the linear polarization of the scattered photons in the present experiments enabled for the first time unambiguous parity assignments in a completely model independent way also to weaker excitations, and hence to study in detail the fragmentation of the orbital $M1$-strength. As an example the results

Energy Resolution ΔE_γ	$\approx$	2.2	keV	at	1332	keV
Total Detection Efficiency ε_{total}	$\approx$	25	%	at	1332	keV
Coincidence Efficiency $\epsilon_c = (H+V)/Total$	$\approx$	25	%	at	3	MeV
Apparative Asymmetry	$\lesssim$	1	%	at	2-4	MeV
Polarization Sensitivity Q	$\approx$	20	%	at	0.5	MeV
	$\approx$	9.5	%	at	4.4	MeV

Table 2.: Characteristics of the fourfold sectored single crystal Ge-Compton polarimeter.

of the photon scattering experiments on stable even-even Gd and Nd isotopes[31,65] are depicted in Fig.8. It shows a comparison of $\Delta K = 1$ transitions in the well deformed Gadolinium isotopes and those observed in the nuclei of the Neodymium isotopic chain where for the first time the transition from spherical to deformed nuclear shapes could be be studied[65]. In the Gadolinium isotopes[31,66] the M1 transition strengths are concentrated in a narrow group arround 3 MeV and follow the $E_x = 66 \cdot \delta \cdot A^{-1/3}\ MeV$ rule to be expected for the orbital $M1$ mode. The same systematic trend has been observed for the Dy isotopes[67]. On the other hand, in the Neodymium nuclei only for the deformed nucleus ^{150}Nd, the cluster of states at 3 MeV is in agreement with this behaviour. But for the transitional nuclei ^{146,148}Nd, the levels decaying predominantly to the groundstate are spread over the full energy range from 2 to 4 MeV. Furthermore, the transition strength to levels with $K = 1$ is much stronger in the well deformed Gadolinium isotopes.

The positive parities for the group of states near 3 MeV in ^{156}Gd observed in a combined analysis of electron and photon scattering experiments[50] could be assigned from the corresponding (e,e')-form factor measurements. Unfortunately, in ^{158}Gd only the positive parities of the strongest transitions, the narrow doublet (3.192 and 3.201 MeV) not to be resolved in electron scattering, could be established from the form factor behaviour[66]. However, for ^{160}Gd the present polarization measurements[68] allowed to determine the parities of all states around = 3.2 MeV marked by crosses. This result dernonstrates that most of the states in the cluster have the same, positive parity and should be attributed to the orbital $M1$ mode which exhibits a rather pronounced fragmentation. The same conclusion holds for the nucleus ^{150}Nd, where our previous polarization data[29,69] for the three strongest transitions could be confirmed and, additionally, now the positive parities of two further weaker transitions have been determined[18].

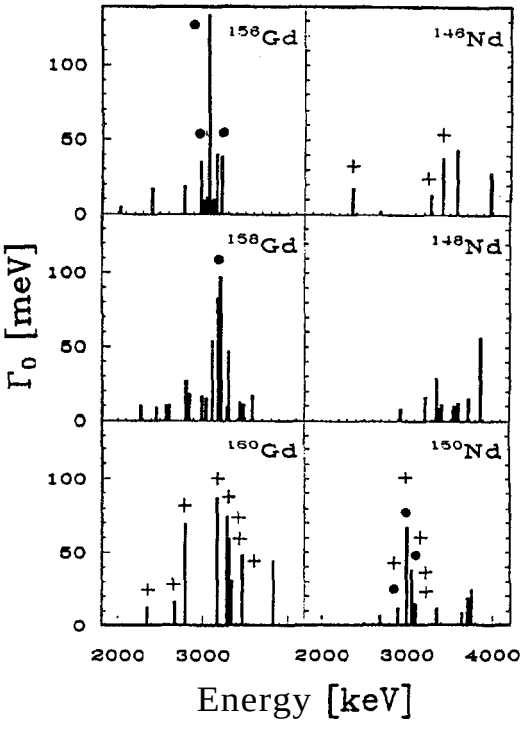

Figure 8: Strength distributions of dipole transitions in the Nd isotopes with decay branching ratios $R_x \leq 1$ in comparison with $\Delta K = 1$ transitions in Gd isotopes attributed to the orbital $M1$ mode (from Refs.[31,65,68,71]. For marked transitions positive parities have been established (full dots: electron scattering data; crosses: photon polarization data).

Recently the Darmstadt group[70] succeeded in a systematic NRF study on the Sm isotopes to show

that the total orbital $M1$ strength increases proportional to the square of the deformation parameter S. The same general trend is also evident in our previous Nd data[65]. For this isotopic chain the polarization experirnents were presently completed by measurements on the transitional nucleus ^{146}Nd[71] to establish safe parity assignments for all Nd isotopes. The observed strong dipole excitations in the transitional nucleus ^{146}Nd have decay branchings which are in surprisingly good agreement with predictions from the Alaga rules valid in the rotational limit. Therefore, in Fig.9 for comparison the strengths of all excitations are added up which show a decay branching $R_{exp} < 1$ corresponding to $\Delta K = 1$ transitions in rotational nuclei, including weak transitions where no parity assignments could be achieved. Fig.9 shows the total strengths added up in the energy range *2-4* MeV observed in the Nd-isotopes (^{142,146,148,150}Nd). Full syrnbols correspond to $M1$ strengths of transitions with reliable parity assignments from our linear polarization measurements or from literature; open symbols correspond to total strengths obtained by adding up the strengths of all dipole transitions in the energy range of interest (E, $= 2-4$ MeV) showing a $R_{exp} \leq 1$ decay branching. The full line represents a fit to the data with determined parities (full symbols, including the ^{148}Nd point). The fact that the full line does not intersect zero is due to the inclusion of the *4095* keV 1^+ state in ^{142}Nd which has the same structure as the 3.97 MeV level in the isotone ^{144}Sm. It should be emphasized that the slope of the linear dependence fitted to the experimental data is strongly influenced by the experimental detection sensitivity (number of added up weak transitions of unknown parities). Consideration of all $\Delta K = 1$ transitions in the energy range of interest (open symbols), which seems to be reasonable in particular in the case of the well deformed nucleus ^{150}Nd, obviously would increase the slope and lead to a remarkable overall agreement with the Darmstadt Sm-results. For comparison the linear dependence on β_2^2 of the total $M1$ strengths observed for the Sm-isotopes in the Darmstadt experiments[70] is plotted as dashed line. Therefore, the new Nd-results represent a reliable independent confirmation of the proposed δ^2 law[70]. This δ^2-dependence of the orbital $M1$ strength originally was predicted by macroscopic models[72,73] and is now explained in microscopic calculations, too[74–76].

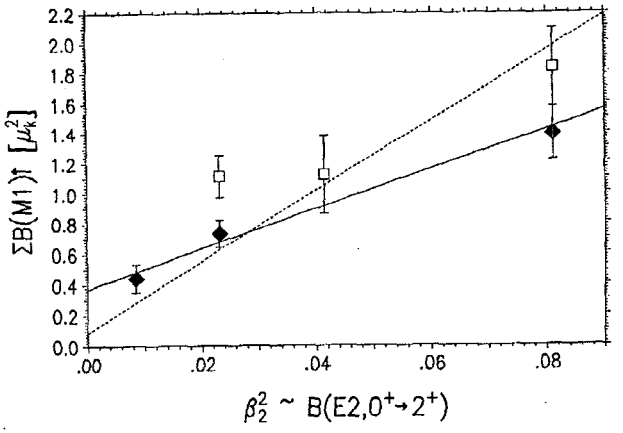

Figure 9: Total $M1$ strength observed in the even Nd isotopes in the energy range 2-4 MeV as a function of the square of the deformation parameter β_2. Full symbols: Only transitions with known parity have been included. Open symbols: Summed strengths of all transitions from spin 1 states with decay branching ratios $R_{exp} \leq 1$ corresponding to K=1 states within the validity of the Alaga rules. The full line represents a fit to the data with determined parities (full symbols, including the ^{148}Nd point) (from Ref.[71]). For comparison the dashed straight line shows the deformation dependence observed by the Darmstadt group for the even Sm isotopes[70].

III.4 Results for E1 excitations in even-even nuclei

The systernatics of $K = 0$, $J = 1^-$ states in rare earth nuclei observed in our previous systematic photon scattering experiments[17] shows that the $K^\pi = 0^-$ strength is mainly concentrated in one or two transitions near *1.5* MeV with summed strengths of C $B(E1)\uparrow \approx 20 \cdot 10^{-3}$ e$^2fm^2$ (corresponding to a rather high value of $\sim 4 \cdot 10^{-3}$ Weisskopf units), whereas the strength at higher energies is rather fragmented. These low lying 1^- states are discussed in terms of K = *0* rotational bands based on an octupole vibration as suggested by Donner and Greiner[77]. This explanation is supported by the observed linear correlation of the energies of the $K = 0$, $J = 1_1^-$ states with the energies of closely lying $J = 3^-$ states[17]. The strengths

of these $K = 0$ $E1$ excitations could be explained by an admixture of the Giant Dipole Resonance (GDR) to these low lying 1^- states[78]. The same description already had been successfully applied for the interpretation of low lying 1^- states in ^{48}Ti, ^{164}Dy, ^{232}Th and ^{238}U observed in (e,e')-experiments[79]. Recently Soloviev et el. [80] described these excitations microscopically within a quasiparticle-phonon model. Von Brentano et al.[81] explained on a quantitative scale both the transition widths Γ_0 and the decay branching ratios of these 1^--states using an improved $E1$ operator within the IBA-sdf-model.

On the other hand, in ^{150}Nd, ^{160}Gd, and ^{162,164}Dy[18,19,82] strong transitions were observed at higher energies near 2.5 MeV, which exhibit decay branching ratios of the corresponding levels indicating K-mixing. The original aim of the present polarization measurements was to determine the parities of these states to search for the proposed enhanced *electric* dipole excitations due to an octupole deformation and/or an α-clustering and to look for a pdssible relation to K-mixing.

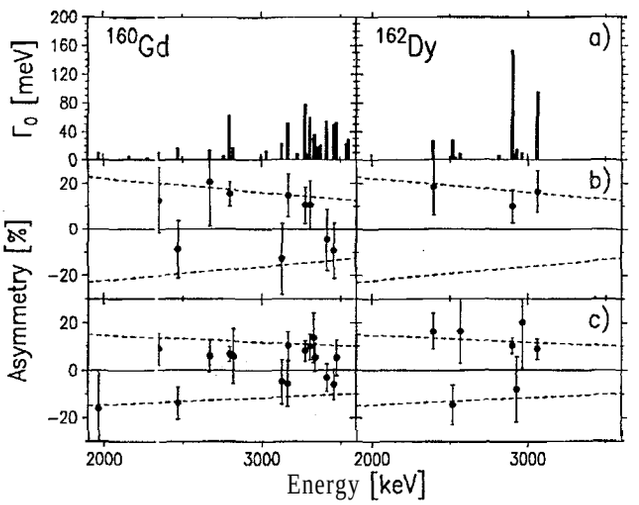

Figure 10: Resilts for ^{160}Gd $(y,\vec{\gamma}')$ and ^{162}Dy $(\gamma,\vec{\gamma}')$: Parts (a): dipole strength distributions. Parts (b): azimuthal asymmetries ε measured by the 5 Ge-detector polarimeter. Parts (c): azimuthal asymmetries ε measured by the sectored Ge-polarimeter. The dashed lines represent the expected asymmetries for $M1$ (positive values) and $E1$ transitions (negative values), respectively (from Ref.[19]).

After the first polarization measurements on ^{150}Nd[65] the neighbouring nuclei ^{160}Gd and ^{162}Dy were investigated. The results are shown in Fig.10. For the first time positive parities could be established for groups of states in the nuclei ^{150}Nd, ^{160}Gd, ^{162,164}Dy. Most of these states are concentrated near 3 MeV and should be attributed to orbital $M1$ excitations (*"Scissors Mode"*). Additionally, enhanced electric dipole excitations in the same deformed nuclei were observed at excitation energies of 2.414, 2.471, 2.520 MeV, and 2.670 MeV, respectively. The transition energies and the enhanced $B(E1)\uparrow$ strengths of 3 to $5\cdot10^{-3}$ e^2fm^2 may suggest an interpretation in terms of the predicted new type of collective electric dipole excitations in deformed nuclei due to reflection asymmetric shapes like octupole deformations and/or cluster configurations. Table 3 summarizes the results and gives a comparison with theoretical estimations, assuming reasonable deformation parameters and cluster admixtures. Both the cluster and the octupole shape models are able to explain at least the right order of magnitude of the observed $E1$ strengths. However, on the basis of the present (γ,γ')-results it is not possible to distinguish between the different excitation mechanisms proposed.

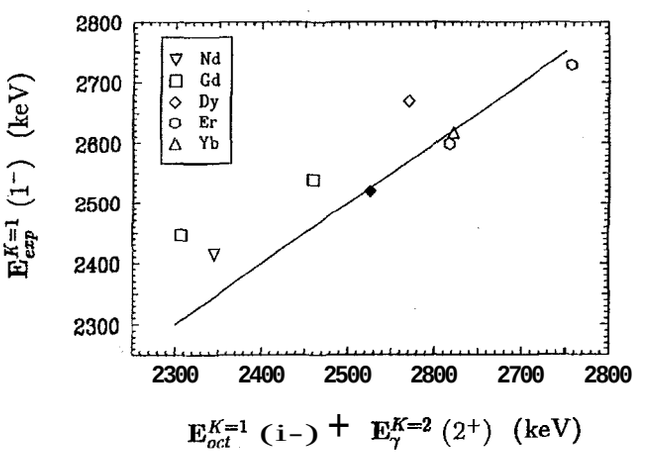

Figure 11: Experimental excitation energies $E^{K=1}_{exp}(1^-)$ of states attributed to a two phonon excitation versus the sum of the $K = 1$ octupole and the y-vibrational excitations $(E^{K=1}_{oct}(1^-) + E^{K=2}_{\gamma}(2^+))$. The full line corresponds to the exact fulfilment of eq.10. In the case of ^{162}Dy (full symbol) all needed energies are experimentally known (from Ref.[82]).

Another very tempting interpretation is to explain these states as two phonon excitations in strongly deformed nuclei caused by the coupling of octupole

Nucleus	E, (MeV)	Γ_0 (meV)	R_{exp}	$B(E1)\uparrow$ $(10^{-3}\ e^2fm^2)$ a-Clust.	Oct.-Def.	Exp.
^{150}Nd	2.414	14.9±2.0	0.86f0.09	1.29	2.9	3.0±0.4
^{160}Gd	2.471	16.4±2.6	1.56±0.21	1.34	3.7	3.1±0.5
^{162}Dy	2.520	30.2±4.0	1.31±0.08	1.15	4.0	5.0±0.4
^{164}Dy	2.670	27.0±4.7	1.14±0.24	0.89	4.1	4.1±0.7

Table 3.: Comparison of experimental results (excitation energies E,, ground state widths Γ_0, decay branching ratios R_{exp} and reduced transition probabilities $B(E1)\uparrow$) for enhanced $E1$ groundstate transitions in deformed rare earth nuclei with model estimations (assuming a cluster admixture of η^2 =0.001 and deformation parameters of β_2 =0.25 and β_3 =0.1, respectively).

vibrations to the $K^\pi = 2^+$, y-vibration. Such two phonon excitations were theoretically already explicitely treated by Donner and Greiner[77] within the Dynamic Collective Model in 1966, but up to now such states could not be detected experimentally. The resulting 1^- states can be excited by dipole transitions from the ground state as a result of the coupling of the giant electric dipole resonance to the octupole vibration[77].

In the following the 1^- states near 2.5 MeV are discussed as possible candidates for such two phonon excitations due to the coupling of quadrupole-y-vibrations ($J = 2^+, K = 2$) and octupole vibrations ($J = 3^-, K = 1$). It is obviously impossible to generate states with J=1 by coupling the y–vibration to octupole excitations with ($J = 3-, K = O$). Octupole vibrations in deformed nuclei and their strong coupling to the deformed quadrupole spheroid were treated in detail by Donner and Greiner[77]. In their work it is shown that the energy of the two phonon excitation is simply given by the sum of the phonon energies in the examined case where K=1 and J_3=1 (J_3= third component of the octupole angular momentum):

$$E_{2Ph}^{K=1}(1^-) = E_{oct}^{K=1}(1^-) + E_{\gamma}^{K=2}(2^+). \qquad (10)$$

The informations on the position of the octupole vibrational bandheads with K=1 are rather sparse. Therefore one has to assume in most cases that the first J^π=1$^-$ state following the K=0 octupole vibrational bandhead is a K=1 state. As possible candidates for the two phonon excitation besides the 1^- states in the four isotopes ^{150}Nd,^{160}Gd, and ^{162,164}Dy investigated so far by polarization measurements the lowest J=1 states above the octupole vibrational bandheads exhibiting an uncommon decay branching ratio have been taken. An excellent agreement between the excitation energies $E_{exp}^{K=1}(1^-)$ of the assumed two phonon excitations and the sum of the $K = 1$ octupole and the γ-vibrational excitations (according to eq. 10) can be stated. Fig.11 illustrates this fact in graphical form.

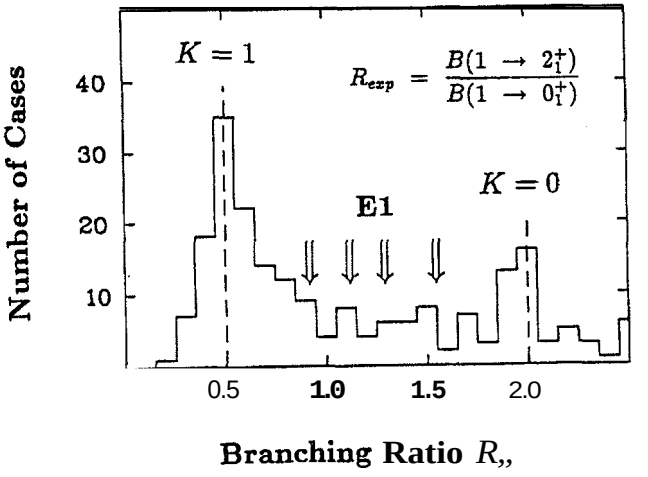

Figure 12: Frequency distribution of experimental decay branching ratios $R_{exp} = B(1 \rightarrow 2_1^+)/B(1 \rightarrow 0_1^+)$ [14,83]. The decay branching ratios for the four $J^\pi = 1^-$ states (enhanced El-excitations) in ^{150}Nd, ^{160}Gd, and ^{162,164}DY discussed in the text are indicated by arrows.

In order to gain more information about the observed 1^- states calculations in the framework of the sdf-IBA model have been performed[82], which support the interpretation as two phonon excitations. Therefore, the observed strong $E1$ excitations near 2.5 MeV in deformed nuclei exhibiting an uncommon decay

branching may be attributed to a two phonon excitation caused by the coupling of the octupole and y-quadrupole vibrations. This conclusion is based on the nearly quaritita tive agreement of the experimental excitation energies with the sum of the $K = 1$ octupole and $K = 2$ y-vibration as suggested by the collective model and on the results of sdf-IBA calculations which reproduce the experimental energies and the structure of the states. However, the sdf–IBA fails to account for the enhanced $B(E l)$values. To obtain more information on the structure of these states it is important to get additional experimental data on the octupole vibrational bands as well as on higher-lying dipole excitations.

It should be emphasized that the $J^{\pi} = 1^{-}$ states corresponding to the enhanced $E1$ excitations near 2.5 MeV in the neighbouring nuclei ^{150}Nd, ^{160}Gd, ^{162}Dy, and ^{164}Dy as discussed above exhibit a decay branching ratio R_{exp} tleviating from the expected values for pure $K = 0$ and $I' = 1$ states and therefore hint to a possible K-mixing[83]. This fact is demonstrated in Fig. 12 where the experimental branching ratios R_{exp} of about *200* transitions in well deformed nuclei are compared with the predictions of the Alage rules[83,14]. One notes two maxima corresponding to $R_{exp} = 0.5$ for $K = 1$ and $R_{exp} = 2$ for $K = 0$. However, some branching ratios lie in between the expectation values and suggest a possible K-mixing. It is of interest to study in future in more detail the occurrence of K-mixing in these strong $E1$ transitians.

III.5 Results for odd-A nuclei

III.5.1 Scissors mode in deformed, odd-A nuclei?

As discussed above there exists detailed information on the clistribution of low-lying electric and in particular of magnetic dipole strength in heavy deformed even-even nuclei. The $M1$ strength concentrated near 3 MeV excitation energy is predominantly of orbital character and is attributed to the so called *"Scissors Mode"*. The Darmstadt group very recently reported on a first search for low-lying $M1$ strength in the heavy, odd nucleus ^{165}Ho. However, no strong transition with $B(M1) \uparrow \geq 0.1\mu_N^2$ could be detected in the energy range near 3 MeV[84].

For the first nuclear resonance fluorescence experiment on an odd mass nucleus performed at the Stuttgart facility ^{163}Dy was chosen as a first candidate[20], since the neighbouring even-even nuclei ^{162}Dy and ^{164}Dy are well investigated[22]. In both isotopes the orbital $M1$ strength is concentrated within two or three strong transitions, in ^{164}Dy the largest $M1$ strength in all rare earth nuclei was observed. Furthermore, detailed spectroscopic information from (n, y), (n, n'y), (d, p), and (d, t) reaction studies[85] is available for this isotope. In addition, orbital $M1$ excitations should be more pronounced in neutron-odd isotopes following theoretical considerations[86].

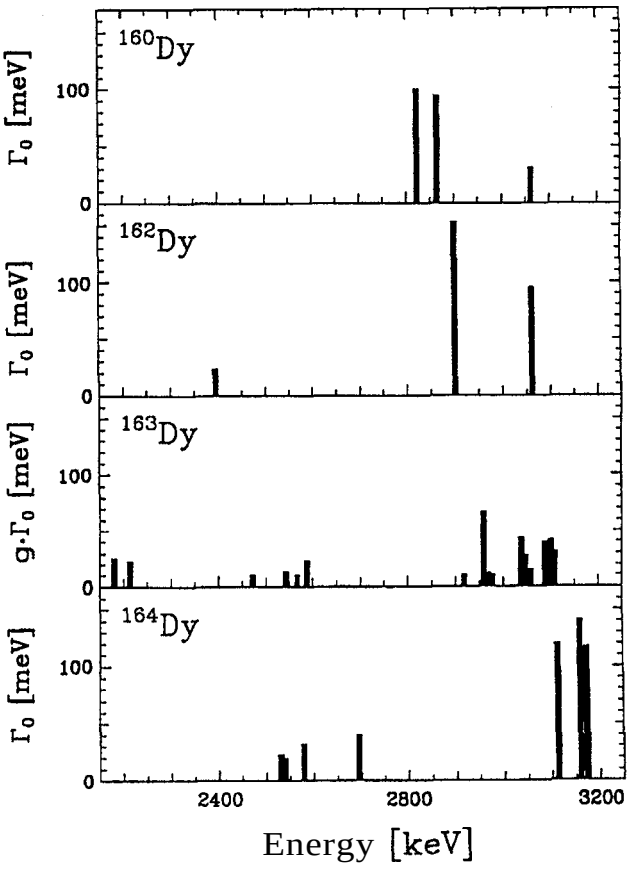

Figure 13: Dipoie strength distribution in ^{163}Dy [20] in comparison with that in even–even Dy isotopes obtained in previous NRF measurements[67].

The resulting dipole strength distribution in the energy range of the orbital $M1$ mode is shown in Fig.13 together with the data for the neighbouring even-even nuclei[22]. The $M1$ character of the excita-

tions in ^{162,164}Dy is known from (e,e')[87] and (y,$\vec{\gamma}$') experiments[18,88]. Unfortunately, the spins of the excited levels in ^{163}Dy cannot be determined unambiguously from this measurement because of the nearly isotropic angular distributions for excitations from the $J^\pi = 5/2^-$ ground state in ^{163}Dy. Therefore, the product of ground state decay width Γ_0 and spin factor $g = (2J+1)/(2J_0+1)$ (in this case 2/3, 1 or 4/3) is plotted.

The observed concentration of dipole strength in ^{163}Dy around 3 MeV fits very well in the sytematics of the scissors mode in the even Dy isotpes. Both the excitation energy as well as the summed strength (assuming an average spin factor g=1) follow the trends expected for the orbital $M1$ mode. The strength distribution is in good agreement with recent calculations performed in the framework of the IBFM-approach (Interacting-Boson-Fermion-Model)[20]. The different decay branchings predicted by the IBFM-calculations for several states can be used for tentative spin assignments.

III.5.2 Dipole excitations in Odd-A, spherical nuclei

Multiphonon excitations have been studied intensively in the last years in many experimental and theoretical investigations. In nuclei with a spherical shape a multiplet of two phonon states with $J^\pi = 1^-, 2^- \ldots 5^-$ should arise due to a coupling of a 3^- octupole and a 2^+ quadrupole vibration. In photon scattering experiments the 1^- member of the $2^+ \otimes 3^-$ multiplet has been found in various N = 82 isotones[89,90,91,65]. In ^{142}Nd an isolated $E1$ transition from a 1^- state at 3425 keV was detected in photon scattering experiments[91,65]. This energy is close to the sum of the 2^+ and 3^- vibrations at 1576 and 2084 keV, respectively. In a recent experiment[21] performed at the bremsstrahlung facility of the Stuttgart Dynamitron accelerator the coupling of an additional neutron to the $2^+ \otimes 3^-$ multiplet has been investigated. In the case of ^{143}Nd the additional neutron occupies the $f_{7/2}$ subshell. Because of the coupling of the odd neutron the five levels of the $2^+ \otimes 3^-$ multiplet in the core nucleus split into 31 levels in ^{143}Nd. Out of these, due to selection rules, in photon scattering experiments only states with spins 5/2, 7/2, and 9/2 can be excited from the groundstate (in total 15 levels). It is clear that one needs an experimental method which is selective in strength and spin to detect these fragmented two-phonon particle levels in the energy range around 3 MeV where the overall level density is already high. The photon scattering method fulfils these requirements.

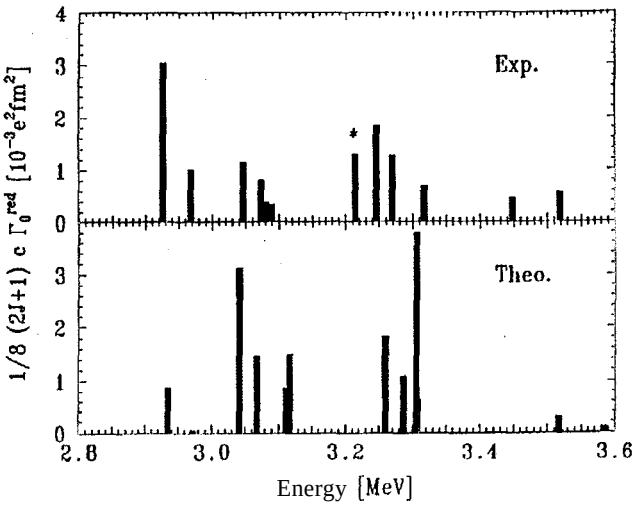

Figure 14: Experimental (upper part) and theoretical (lower part) dipole strength distribution in ^{143}Nd between 2.8 and 3.6 MeV[21]. If the transitions have an $E1$ character one finds for the plotted quantity $\frac{1}{8}(2J+1) \cdot c \cdot \Gamma_0^{red} = B(E1; J \rightarrow J_0)\downarrow$ (with $\Gamma_0^{red} = \Gamma(J \rightarrow J_0) \cdot E_\gamma^{-3}$ and $c = 0.9553 \cdot 10^{-3}$ e^{2}fm^2 MeV^3/meV). The level marked by an asterisk shows a strong branching to the $3/2^-$ level at 742 keV and is not expected to be reproduced by the theoretical calculations[21].

The measured strength distribution[21] is shown in Fig.14 (upper part). The assumption of electric dipole character for these transitions is highly favourable from the known dipole excitations in the neighbouring nuclei. The total $B(E1)\downarrow$ strength observed in ^{143}Nd (deexcitation of J=5/2, 7/2, and 9/2 states) amounts to about three times the strength of the strong 3452 keV transition in the even core nucleus ^{142}Nd. The fact that the sum rule is fulfilled proofs the two-phonon $\otimes$ particle structure for the excitations in ^{143}Nd.

In the lower part the experimental results are compared with calculations. These model calculations[21] consists of two parts. First the prominent collective features of the core nucleus (energetic positions of the $2^- \ldots 5^-$ members of the multiplet) are described

in the framework of the sdf-IBM. Then the coupling of the additional neutron is calculated using the code COUPLIN[92]. The calculated distribution (lower part of Fig.14) is quite similar to the experimental one. The agreement between the experimental data and the core coupling calculations can be considered to be a strong argument in favour of the proposed $2^+ \otimes 3^- \otimes$ particle structure of the observed states near 3 MeV.

IV. Summary and outlook

In this report two topics, low energy photofission and photon scattering experiments, are discussed. Fragment angular distributions reveal, as well known, direct information on the spectrum of the transition states and hence on collective excitations at the large deformations of the fission barriers. Essential progress could be achieved in the last years. The most exciting, novel result of recent experiments was the observation of a mass dependence of fission fragment angular distribiitions. First (e, el$f$)-coincidence experiments allowed to disentangle all six transition channels in ^{238}U and demonstrated the power of this method using monochromatic virtual photons. Unfortunately, data exist only for this isotope and, furthermore, the statistics in these experiments did not allow to make diverse mass cuts. Monochromatic, tagged real photons, for intensity reasons, up to now only could be applied for the investigation of fragment angular distributions in the second chance fission of ^{238}U, where the higher cross sections compensate for the low photon flux. In principle, the use of linearly polarized photons offers considerable advantages. However, only *continuous* polarized off-axis bremsstrahlung was available in first experiments. Therefore, for future photofission experiments there is a strong demand for first investigations with monochromatic, if possible polarized photons. As already pointed out all effects observed so far in bremsstrahlung experiments will be considerably enhanced in nieasurements using monochromatic photons. A centra subject of future experiments will be the study of the ccupling of the Bohr transition states, settling the angular distributions, to diverse fission modes, determining tlie fragment mass and energy distributions. Therefore, simultaneous measurements of both, angular and mass distributions seem to be indispensable.

The photon scattering method (NRF experiments) using intense CW bremsstrahlung beams has proven its outstanding capability to investigate low lying magnetic and electric dipole excitations in heavy nuclei. However, it should be noted that parity assignments are of crucial importance for the interpretation of the data. Parities can be determined as discussed above in time consuming measurements of the linear polarization of the scattered photons using Compton polarimeters. For higher excitation energies ($E \geq 5$ MeV), like for the search for $M1$ spin flip strength, the use of polarized photons in the entrance channel is more favourable. Therefore, high flux sources of linearly polarized photons are highly desirable. There are many open questions in nuclear structure physics, partially raised by the recent experiments, which can be tackled by future NRF experiments. However, it should be emphasized that a deeper insight into the underlying structure of the states excited by real photons comes from the comparison with results obtained by different probes. In particular (e, e')-form factor measurements and (p, p')-experiments are of importance in this respect.

As stated in the beginning, powerful low energy CW electron accelerators are necessary to provide the photon sources needed in the experiments discussed here. After setting to work the 855 MeV stage of the Mainz Microtron $MAMI\ B$[93] the 185 MeV electron beam is no more available for further (e, $e'f$)-coincidence experiments. A suitable facility for such experiments, however, exist at the new 130 MeV superconductive $S-DALINAC$ at Darmstadt[94,95]. (including a modern large solid angle electron spectrometer). At the injector section of the $S-DALINAC$ (10 MeV) NRF experiments very successfully have been performed[96]. Due to the limited achievable current of $\approx 20\ \mu$A and the narrow geometry this experimental set up is not well suited to produce polarized off-axis bremsstrahlung. A new polarized off-axis bremstrahlung facility recently has been built at the 15 MeV high current e^--linac at Gent ($\bar{I} \approx 2$ mA)[25]. The duty cycle of the Gent ma-

chine is limited to about 2%, nevertheless, this new facility devoted to NRF experiments brought a considerable progress compared to the old Giessen set up (duty cycle 0.12%)[25]. The Stuttgart Dynamitron as an electrostatic accelerator delivers very high electron CW currents (up to 4 mA), however, is limited in its maximum energy to 4.3 MeV. At the present time there is, at least to my knowledge, no low energy tagged, polarized photon facility in operation. Therefore, I see good perspectives for the new 30 MeV microtron under construction at the University of São Paulo.

Acknowledgements

The experiments reported on have been performed during the last years by our Stuttgart and former Giessen photonuclear group in collaborations with the groups of Prof's P. von Brentano (Koln), L.S.Cardman (Urbana), K.T.Knöpfle (Heidelberg), A.M.Nathan (Urbana), A.Richter (Darmstadt), and M.Schumacher (Gottingen). It is a pleasure for me to thank all colleagues for the very fruitful and stimulating collaboration and for their really essential contributions to results presented in this report. Special thanks are due to my longterm Stuttgart and Giessen collaborators R.D.Heil, J.Margraf, H.H.Pitz, F.Steiper, Th.Weber, C.Wesselborg, W.Wilke, and A.Zilges, R.-D.Herzberg (Koln) for their outstanding engagement and enthusiasm which enabled the realization of the various projects. The extensive and continuous financia1 support by the Deutsche Forschungsgemeinschaft is gratefully acknowledged.

References

1. H. Überall, Electron Scattering *from* Complex Nu*clei* (Academic, New York, 1971) .
2. L. W. Fagg and S. S. Hanna, Rev. Mod. Phys. 31, 711 (1957).
3. T. W. Donnelly and J. D. Walecka, Ann.Rev.Nucl.Sci. 25, 329 (1975).
4. Th. Weber et al., Nucl.Phys. **A510**, 1 (1990).
5. R. Vandenbosch and J.R. Huizenga, Nuclear *Fis*sion (Academic, New York, 1973).
6. E. Jacobs and U. Kneissl, Photon- ***and*** Electron-Induced Fission in The Nuclear Fission Process, edited by C. Wagemans (CRC PRESS INC, Boca Raton, 1991).
7. W. Wilke et al., Phys. Lett. **207B**, 385 (1988).
8. W. Wilke et al., Phys.Rev. C42, 2148 (1990).
9. F. Steiper et al., Nucl.Phys. **A563**, 282 (1993).
10. A. Bohr, Proc. of 1^{st} UN Int. Conf. on Peacefui Uses of **At.** Energy, Vol.I, p.151, New York (1956).
11. U. Brosa et al., Physics Reports 197, 167 (1990).
12. D. Bohle et al., Phys.Lett. **137B**, 27 (1984).
13. A. Richter, Nucl.Phys. **A507**, 99c (1990).
14. A. Richter, Nucl.Phys. **A522**, 139c (1991).
15. U. Kneissl, Prog.Part.Nucl.Phys. 24, 41 (1990).
16. U. Kneissl, Prog.Part.Nucl.Phys. 28, 331 (1992).
17. A. Zilges et al., Z.Phys. **A** 340, 155 (1991).
18. H. Friedrichs et al., Phys.Rev. C45, R892 (1992).
19. H. Friedrichs et al., Nucl.Phys. **A553**, 553c (1993).
20. I. Bauske et al., Phys.Rev.Lett. 71, 975 (1993).
21. A. Zilges et al., Phys.Rev.Lett. 70, 2880 (1993).
22. Th. Weber et al., Phys.Lett. **215B**, 469 (1988).
23. H. Herminghaus, Nucl.Instr. Meth. 138, 1 (1976).
24. R. Ratzek et al., Z.Phys. **A308**, 63 (1982).
25. U.E.P. Berg and U. Kneissl, Ann.Rev.Nucl.Part.Sci. 37, 33 (1987).
26. F. Gonnenwein, Nucl.Phys. **A502**, 159c (1989).
27. J. Drexler, J. et al., Nucl.Instr. Meth. Phys. Res. 220, 409 (1984).
28. W. Wilke et al., Nucl.Instr. Meth. Phys. Res. **A272**, 785 (1988).
29. R.D. Heil et al., Nucl.Phys. **A506**, 223 (1990)
30. B. Schlitt et al., Nucl.Instr. Meth. Phys. Res. **A337**, 416 (1994).
31. H.H. Pitz et al., Nucl.Phys. **A492**, 441 (1989).
32. P.A. Dickey and P. Axel, Phys.Rev.Lett. 35, 501 (1975).
33. L.J. Lindgren et al., Nucl.Phys. **A298**, 43 (1978).
34. L.J. Lindgren et al., Z.Phys. **A285**, 415 (1978).
35. J.D.T. Arruda-Neto et al., Nucl.Phys. **A389**, 378, 1982).

36. S. Bjørrholm and J.E. Lynn, Rev.Mod.Phys. 52, 725,(1980).
37. D. Zawischa and J. Speth, Lecture Notes in Physics **158**, 231 (1982).
38. R. De Eeo et al., Nucl.Phys. 8441, 591 (1985).
39. N.S. Rabotnov et al., Sov.J.Nucl.Phys. 11, 285 (1970).
40. R. Vandenbosch, Phys.Lett. **45B**, 207 (1973).
41. J. Blons et al., Nucl.Phys. **A414**, 1 (1984).
42. A.S. Soldatov et al, Sov.J.Nucl.Phys. **11**, 552 (1970).
43. O. Hittmair, Nucl. Phys. 18, 346 (1960).
44. J.A. Wheeler, Fast Neutron Physics, edited by J.B. Marion and R. Fowler, (Interscience, New York, 1963) vol. 2, p. 2051.
45. V.V. Flambaum, Sov. J. Nucl. Phys. 42 (1985) 366
46. F.-M. Baumann et al., Nucl. Phys. **A502**, 271c (1989).
47. G.A. Leander et al., Nucl.Phys. **A453**, 58 (1986).
48. P.A. Butler and W. Nazarewicz, Nucl.Phys. **A533**, 249 (1991).
49. F. Iachello, Phys. Lett. **160B**, 1 (1985).
50. D. Bohlt: et al., Nucl.Phys. **A458**, 205 (1986).
51. G. Alaga et al., Dan.Mat.Fys.Medd. 29, 1 (1955).
52. P.M. Endt et al., Nucl.Phys. **A310**, 1 (1978).
53. H. Maser, Diploma Thesis, Stuttgart (1993), unpublished
54. R.D. Heil et al., Nucl.Phys. **A476**, 39 (1988).
55. J. Margraf et al., Phys.Rev. C42, 771 (1990).
56. N.Lo Iuclice et al., Phys.Rev.Lett. 41, 153 (1978).
57. A.E.L. Dieperink et al., Ann.Rev.Nucl.Part.Sci. 35, 77 (1985).
58. I. Hamamoto et al., Phys. Lett. **145B**, 163 (1984).
59. K. Sugawara et al., Phys. Lett. **206B**, 578 (1988).
60. A. Faessler et al., Nucl.Phys. **A515**, 237 (1990).
61. C. de Ccster et al., Nucl.Phys. **A524**, 441 (1991).
62. C. de Ccster et al., Nucl.Phys. **A529**, 507 (1991).
63. D. Zawischa et al., Z.Phys. **339A**, 97 (1991).
64. A. Faessler, Prog.Part.Nucl.Phys. 28, 341 (1992).
65. H.H. Pita et al., Nucl.Phys. **A509**, 587 (1990).
66. U. Hartmann et al., Nucl.Phys. A499 93 (1989).
67. C. Wesselborg et al., Phys. Lett. **207B**, 22 (1988).
68. H. Friedrichs et al., Nucl.Phys. **A567**, 266 (1994).
69. B. Kasten et al, Phys.Rev.Lett. 63, 609 (1989).
70. W. Ziegler et al., Phys.Rev.Lett. 65, 2515 (1990).
71. J. Margraf et al., Phys.Rev. C47, 1474 (1993).
72. S.G. Rohozitíski and W.Greiner, Z.Phys. **322A**, 271 (1985).
73. R. Nojarov et al., Z.Phys. **124A**, 289 (1986).
74. I. Hamamoto et al., Phys. Lett. **260B**, 6 (1991).
75. E. Garrido et al., Phys.Rev. C44, R1250 (1991).
76. R.R. Hilton et al., Phys.Rev. C47, 662 (1993).
77. W. Donner and W. Greiner, Z.Phys. 197, 440 (1966).
78. A. Zilges et al., Z.Phys. **A341**, 440 (1992).
79. Th. Guhr et al., Nucl.Phys. **A501**, 95 (1989).
80. V.G. Soloviev and A.V. Sushkov, Phys. Lett. **262B**, 189 (1991).
81. P. von Brentano et al., Phys. Lett. **278B**, 221 (1992).
82. U. Kneissl et al., Phys. Rev. Lett 71 2180 (1993).
83. A. Zilges et al., Phys.Rev. **C42**, 1945 (1990).
84. N. Huxel et al., Nucl.Phys. **A539**, 478 (1992).
85. H.H. Schmidt et al., Nucl.Phys. **A504**, 1 (1989).
86. P. van Isacker et al., Phys. Lett. **225B**, 1 (1989).
87. D. Bohle et al., Phys. Lett. **148B**, 260 (1984) and Phys. Lett. **195B**, 326 (1987).
88. J. Margraf et al., to be published.
89. F.R. Metzger, Phys.Rev. C14, 543 (1976).
90. F.R. Metzger, Phys.Rev. C18, 2138 (1978).
91. F.R. Metzger, Phys.Rev. **C18**, 1603 (1978).
92. F. Dönau and S. Frauendorf, Phys. Lett. **71B**, 263 (1977); F. Dönau, Z.Phys. **A293**, 31 (1979).
93. H. Herminghaus et al., Proceedings of the 1990 Linear Accelerator Conference, Albuquerque (New Mexico), 362 (1990).
94. K. Alrutz-Ziemssen et al., Proceedings of the 1990 Linear Accelerator Conference, Albuquerque (New Mexico), 662 (1990).
95. A. Richter, Nucl. Phys. News **1**, 20 (1990).
96. K. Govaert et al., Nucl.Instr. Meth. Phys. Res. **A337**, 265 (1994).